Annales Geophysicae, 23, 799–808, 2005
SRef-ID: 1432-0576/ag/2005-23-799

Annales Geophysicae

Magnetosphere-ionosphere coupling currents in Jupiter's middle magnetosphere: effect of magnetosphere-ionosphere decoupling by field-aligned auroral voltages

J. D. Nichols and S. W. H. Cowley

Department of Physics and Astronomy, University of Leicester, Leicester LE1 7RH, UK

Received: 23 August 2004 – Revised: 10 November 2004 – Accepted: 15 December 2004 – Published: 30 March 2005

Abstract. We consider the effect of field-aligned voltages on the magnetosphere-ionosphere coupling current system associated with the breakdown of rigid corotation of equatorial plasma in Jupiter's middle magnetosphere. Previous analyses have assumed perfect mapping of the electric field and flow along equipotential field lines between the equatorial plane and the ionosphere, whereas it has been shown that substantial field-aligned voltages must exist to drive the field-aligned currents associated with the main auroral oval. The effect of these field-aligned voltages is to decouple the flow of the equatorial and ionospheric plasma, such that their angular velocities are in general different from each other. In this paper we self-consistently include the field-aligned voltages in computing the plasma flows and currents in the system. A third order differential equation is derived for the ionospheric plasma angular velocity, and a power series solution obtained which reduces to previous solutions in the limit that the field-aligned voltage is small. Results are obtained to second order in the power series, and are compared to the original zeroth order results with no parallel voltage. We find that for system parameters appropriate to Jupiter the effect of the field-aligned voltages on the solutions is small, thus validating the results of previously-published analyses.

Keywords. Magnetospheric physics (current systems; magnetosphere-ionosphere interactions; planetary magnetospheres)

1 Introduction

The physics of Jupiter's middle magnetosphere is dominated by the source of sulphur and oxygen plasma originating from the moon Io (e.g. Siscoe and Summers, 1981; Hill et al., 1983; Belcher, 1983; Vasyliunas, 1983; Bagenal, 1994; Delamere and Bagenal, 2003). Particle pick-up and centrifugally-driven outflow result in sub-corotation of this plasma, which bends the field lines out of magnetic meridian planes, and sets up the large-scale current system shown in Fig. 1 (Hill, 1979; Huang and Hill, 1989; Dougherty et al., 1993; Pontius, 1997; Bunce and Cowley, 2001; Khurana, 2001). This current system communicates atmospheric torque to the magnetospheric plasma, and is directed equatorward in the ionosphere, radially outward in the equatorial plane, and closes via field-aligned currents flowing outward in the inner region and inward in the outer region. Current calculations were performed for a dipole field by Hill (2001), and for both a dipole and current sheet field by Cowley and Bunce (2001), Cowley et al. (2002, 2003), and Nichols and Cowley (2003). For plasma mass outflow rates of $\sim$1000 kg s^{-1} and ionospheric Pedersen conductivities of a few tenths of a mho, the peak upward field-aligned currents in the ionosphere were calculated to be a few tenths of a μA m^{-2}, in agreement with empirical estimates based on magnetospheric magnetic field data (Bunce and Cowley, 2001; Khurana, 2001). Bunce and Cowley (2001) and Cowley and Bunce (2001) also showed that in the tenuous high-latitude Jovian environment such field-aligned currents exceed those that can be carried by precipitating hot magnetospheric electrons, thus requiring the existence of field-aligned voltages. These were computed using Knight's (1973) kinetic theory, with electron source plasma parameters derived from Voyager data. The calculations of Cowley and Bunce (2001) and Cowley et al. (2002, 2003) yielded field-aligned voltages of $\sim$25–100 kV for typical parameters, sufficient to produce precipitating electron energy fluxes of up to several tens of mW m^{-2}, thus leading to 'main oval' auroras of up to several hundred kR in brightness, comparable to observed intensities (e.g. Satoh et al., 1996; Prangé et al., 1998; Clarke et al., 1998; Vasavada et al., 1999; Pallier and Prangé, 2001; Grodent et al., 2003). Most recently, Nichols and Cowley (2004) have also self-consistently included the effect of precipitation-induced enhancement of the ionospheric Pedersen conductivity.

One key feature of all these calculations, however, is the assumption of perfect mapping of the electric field and

Correspondence to: J. D. Nichols
(jdn@ion.le.ac.uk)

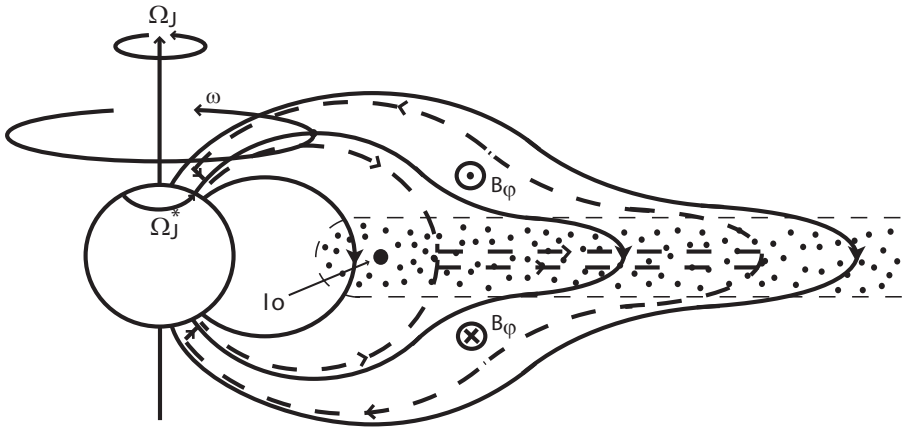

Fig. 1. Sketch of a meridian cross section through Jupiter's inner and middle magnetosphere, showing the principal physical features involved. The arrowed solid lines indicate magnetic field lines, the arrowed dashed lines the magnetosphere-ionosphere coupling current system, and the dotted region the rotating disc of out-flowing iogenic plasma (From Cowley and Bunce, 2001).

plasma flow along equipotential field lines between the equatorial plane and the ionosphere. The associated field-aligned voltages were then calculated from the field-aligned current using Knight's (1973) theory. In principle, however, the field-aligned voltage modifies the mapping of the electric field, and hence the plasma flow, between the two regions. This lack of internal consistency was discussed briefly by Cowley and Bunce (2001), who argued that the effect is likely to be small, since field-aligned voltages of ∼25–100 kV are small compared with field-perpendicular voltages across the middle magnetosphere of the order of several MV. However, to date no self-consistent calculation has been performed which quantifies the effect of the parallel voltage on the flow and current system, such that this argument has remained untested. In view of the significance of these processes for Jovian middle magnetosphere physics, it is important to quantify these effects within a self-consistent calculation, and hence to determine whether previously-presented results are indeed valid. In this paper we derive a theory which, for the first time (to our knowledge), self-consistently incorporates the field-aligned voltage into the calculation. This theory is then applied to the Jovian middle magnetosphere, and results are compared with those previously derived.

2 Governing equations

In this section we summarise the equations which govern the system, the main new feature being the self-consistent inclusion of the field-aligned voltage calculated from Knight's (1973) kinetic theory. In other aspects, however, the analysis follows those given previously by Hill (1979, 2001), Pontius (1997), Cowley et al. (2002, 2003), and Nichols and Cowley (2003), such that only the main results will be outlined, together with the approximations and assumptions made. We begin with a description of the magnetic field model which serves as the essential background to the problem.

2.1 Magnetic field model

The magnetic field model is that used previously by Nichols and Cowley (2004). The field is assumed to be axisymmetric, as appropriate to Jupiter's middle magnetosphere, such that the poloidal components can be described by a flux function $F(\rho, z)$, related to the magnetic field by

$$\boldsymbol{B} = \left(\frac{1}{\rho}\right) \nabla F \times \hat{\varphi}, \tag{1}$$

where ρ is the perpendicular distance from the magnetic axis, z is the distance along this axis from the magnetic equator, and φ is the azimuthal angle. Function F is then constant along a given field line, such that mapping between the equatorial plane and the ionosphere is obtained simply from writing $F_e{=}F_i$. Assuming the ionospheric field is purely dipolar and neglecting any small effects due to magnetospheric currents, the ionospheric flux function is

$$F_i = B_J \rho_i^2 = B_J R_J^2 \sin^2 \theta_i, \tag{2}$$

where B_J is the dipole equatorial magnetic field strength (equal to 426 400 nT in conformity with the VIP 4 internal field model of Connerney et al., 1998), R_J is Jupiter's radius (71 323 km), ρ_i is the perpendicular distance from the magnetic axis, and θ_i is the magnetic co-latitude. The absolute value of F is fixed by setting $F{=}0$ on the magnetic axis. The flux function in the equatorial plane is found by integrating

$$B_{ze} = \frac{1}{\rho_e} \frac{dF_e}{d\rho_e}, \tag{3}$$

where B_{ze} is the north-south magnetic field threading the equatorial plane

$$B_{ze}(\rho_e) = -\left\{ B_0 \left(\frac{R_J}{\rho_e}\right)^3 \exp\left[-\left(\frac{\rho_e}{\rho_{e0}}\right)^{5/2} \right] + A \left(\frac{R_J}{\rho_e}\right)^m \right\}, \tag{4a}$$

where B_o=3.335×10^5 nT, ρ_{eo}=14.501 R$_J$, A=5.4×10^4 nT, and m=2.71. This field is close to that employed by Cowley and Bunce (2001) and Cowley et al. (2002, 2003), who used the 'Voyager-1/Pioneer-10' model of Connerney et al. (1981) (the 'CAN' model) in the inner region, and the Voyager-1 model of Khurana and Kivelson (1993) (the 'KK' model) at large distances. The second term in Eq. (4a) is simply the latter model, while the first is a modified dipole field. The corresponding equatorial flux function is

$$F_e(\rho_e) = F_\infty + \frac{B_0 R_J^3}{2.5\rho_{e0}}\Gamma\left[-\frac{2}{5}, \left(\frac{\rho_e}{\rho_{e0}}\right)^{5/2}\right] + \frac{A}{(m-2)}\left(\frac{R_J}{\rho_e}\right)^{m-2}, \quad (4b)$$

where $F_\infty \approx 2.841\times10^4$ nT R$_J^2$ is the value of the flux function at infinity, and $\Gamma(a,z)$ is the incomplete gamma function $\Gamma(a,z) = \int_z^\infty t^{a-1}e^{-t}dt$. The ionospheric mapping between the equatorial plane and the ionosphere is then given from Eq. (2) by

$$\sin\theta_i = \sqrt{\frac{F_e(\rho_e)}{B_J R_J^2}}, \quad (5)$$

such that the field line passing through the equatorial plane at the outer edge of the model at 100 R$_J$ maps to ∼15.7° in the ionosphere. Figure 2 shows $|B_{ze}|$, F_e, and θ_i versus ρ_e, over the range 0 to 100 R$_J$. The solid lines show the above model, while the long-dashed lines show the dipole values for comparison. The dotted lines in panel (a) also show the values for the CAN/KK models, which are projected beyond their intersection for ease of visibility. The horizontal dotted lines in panels (b) and (c) show the asymptotic values of F_e and θ_i at large distances.

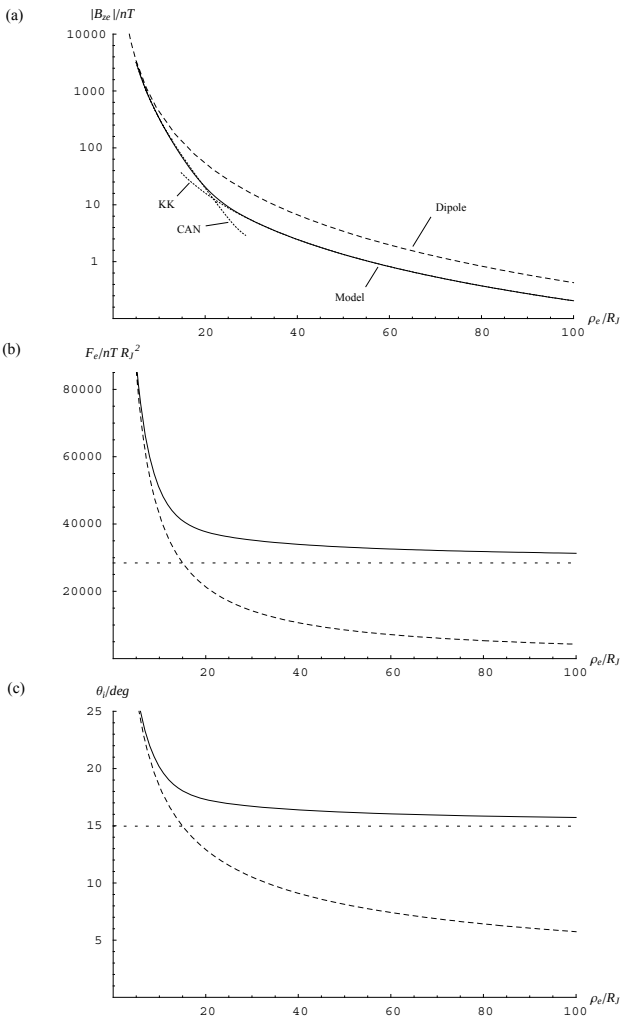

Fig. 2. Plots showing the parameters of the current sheet field model employed in this paper (solid lines) compared with values for the planetary dipole field alone (dashed lines). Plot **(a)** is a log-linear plot of the modulus of the north-south component of the equatorial magnetic field $|B_{ze}|$ in nT threading the equatorial plane, shown versus Jovicentric equatorial radial distance ρ_e. We note that the actual values are negative (i.e. the field points south). The solid line shows the field model employed in this paper, given by Eq. (4a), which is based on the CAN-KK model of previous papers. The dotted lines show the CAN and KK models themselves, plotted beyond their intersection for ease of visibility. Plot **(b)** similarly shows the equatorial flux function of the model field F_e in nT R_J^2 versus Jovicentric equatorial radial distance ρ_e, given by Eq. (4b). The horizontal dotted line shows the value of the flux function at infinity F_∞. Plot **(c)** shows the mapping of the field lines between the equatorial plane and the ionosphere, determined from Eq. (4). The ionospheric co-latitude of the field line θ_i is plotted versus Jovicentric equatorial radial distance ρ_e. The horizontal dotted line shows the ionospheric co-latitude of the field line which maps to infinity in the equatorial plane for the current sheet field model.

2.2 Magnetosphere-ionosphere decoupling by field-aligned voltages

The primary new feature of this calculation is the self-consistent inclusion of the field-aligned voltage in the mapping of the electric field and flow between the magnetosphere and ionosphere. It is convenient to use the flux function F as the spatial coordinate, such that the equatorial and ionospheric plasma angular velocities and the field-aligned voltage are given by the functions $\omega_e(F)$, $\omega_i(F)$ and $\Phi_\parallel(F)$, respectively. We assume a steady flow, such that the electric field $\boldsymbol{E}=-\boldsymbol{v}\times\boldsymbol{B}$ can be described by a scalar potential Φ through $\boldsymbol{E}=-\nabla\Phi$. Using Eq. (1) we then find that $\nabla\Phi=\omega\nabla F$, such that

$$\omega_e(F) = \frac{d\Phi_e(F)}{dF} \quad (6a)$$

and

$$\omega_i(F) = \frac{d\Phi_i(F)}{dF}. \quad (6b)$$

Taking the field-aligned voltage to be positive when the ionosphere has a higher potential than the equator (the case for upward-directed electric field and downward precipitating electrons), then

$$\Phi_i(F) = \Phi_e(F) + \Phi_\parallel(F). \quad (7)$$

Differentiating with respect to F and combining with Eqs. (6a, b) yields

$$\omega_i(F) = \omega_e(F) + \frac{d\Phi_\parallel(F)}{dF}. \quad (8)$$

This is the equation which relates the ionospheric and equatorial angular velocities in the presence of a field-aligned voltage, and which we refer to as the magnetosphere-ionosphere decoupling equation.

We must also specify how $\Phi_\parallel$ depends on the conditions present in the magnetosphere. Here, in common with previous work, we use Knight's (1973) kinetic theory. This gives the field-aligned voltage required to drive a field-aligned current $j_{\parallel i}$ that exceeds the maximum value $j_{\parallel i\mathrm{o}}$, that can be carried by unaccelerated precipitating magnetospheric electrons alone. For an isotropic Maxwellian electron source population of density N and thermal energy W_{th} (equal to kT_e), $j_{\parallel i\mathrm{o}}$ is

$$j_{\parallel i\mathrm{o}} = eN\left(\frac{W_{th}}{2\pi m_e}\right)^{1/2}. \quad (9)$$

Under the usual simplifying assumptions (e.g. Cowley and Bunce, 2001), the minimum field-aligned voltage required to drive a current greater than $j_{\parallel i\mathrm{o}}$ is then

$$\Phi_\parallel\left(j_{\parallel i}\right) = \frac{W_{th}}{e}\left[\left(\frac{j_{\parallel i}}{j_{\parallel i\mathrm{o}}}\right) - 1\right]. \quad (10)$$

In principle, $\Phi_\parallel$ will vary with F on differing flux shells due to variations in the source parameters N and W_{th}. However, in the absence of detailed models, here we employ constant values based on Voyager data, i.e. N=0.01 cm^{-3} and W_{th}=2.5 keV, as used in our previous papers (Scudder et al., 1981). In this case $\Phi_\parallel$ varies with F due to variations in $j_{\parallel i}$ only. Substitution of Eq. (10) into Eq. (8) then gives

$$\omega_i(F) = \omega_e(F) + \frac{W_{th}}{ej_{\parallel i\mathrm{o}}}\frac{dj_{\parallel i}}{dF}. \quad (11)$$

This equation is strictly valid only for $j_{\parallel i} \geq j_{\parallel i\mathrm{o}}$. However, this condition is met essentially everywhere in the middle magnetosphere, except in the innermost region where the field-aligned current drops to small values. Here, therefore, we assume that Eq. (11) is valid for all $j_{\parallel i} > 0$, i.e. throughout the middle magnetosphere. This is equivalent to making the approximation

$$\Phi_\parallel\left(j_{\parallel i}\right) \approx \frac{W_{th}}{e}\left(\frac{j_{\parallel i}}{j_{\parallel i\mathrm{o}}}\right) \quad (12)$$

in Eq. (10). We also note that the corresponding precipitating energy flux of accelerated electrons is

$$E_f = \frac{E_{f\mathrm{o}}}{2}\left[\left(\frac{j_{\parallel i}}{j_{\parallel i\mathrm{o}}}\right)^2 + 1\right] \approx \frac{E_{f\mathrm{o}}}{2}\left(\frac{j_{\parallel i}}{j_{\parallel i\mathrm{o}}}\right)^2, \quad (13)$$

a result due to Lundin and Sandahl (1978). In this expression $E_{f\mathrm{o}}$ is the precipitating energy flux of unaccelerated magnetospheric electrons corresponding to field-aligned current $j_{\parallel i\mathrm{o}}$, given by

$$E_{f\mathrm{o}} = 2NW_{th}\left(\frac{W_{th}}{2\pi m_e}\right)^{1/2}. \quad (14)$$

2.3 Current circuit equations

We now outline the calculation of the current system components illustrated in Fig. 1. This is essentially the same as that given previously by Hill (2001), Cowley and Bunce (2001), Cowley et al. (2002, 2003) and Nichols and Cowley (2003, 2004), except that we now specifically use the ionospheric plasma angular velocity ω_i to derive the ionospheric electric field in the rest frame of the neutral atmosphere, and hence the Pedersen and field-aligned currents. The equatorward-directed height-integrated Pedersen current is then

$$i_P = 2\Sigma_P\left(\Omega_J^* - \omega_i\right)\rho_i B_J = 2\Sigma_P^*\left(\Omega_J - \omega_i\right)\rho_i B_J, \quad (15)$$

where Ω_J^* is the angular velocity in the inertial frame of the neutral atmosphere in the Pedersen layer, which is reduced from the planet's angular velocity Ω_J (1.76×10^{-4} rad s^{-1}) due to ion-neutral collisional drag. This slippage can be parameterised by the factor k defined by

$$\left(\Omega_J - \Omega_J^*\right) = k\left(\Omega_J - \omega_i\right), \quad (16)$$

as introduced by Huang and Hill (1989). The value of k is not well known at present, but recent modelling suggests $k\approx0.5$ under Jovian auroral conditions (Millward et al., 2004). Parameter Σ_P^* in Eq. (15) is the effective value of the height-integrated Pedersen conductivity, related to the true value Σ_P by $\Sigma_P^* = (1-k)\,\Sigma_P$. In deriving Eq. (15) we have also assumed that the polar magnetic field is vertical and equal to $2B_J$ in strength.

Current continuity in the circuit shown in Fig. 1 requires $\rho_e i_\rho = 2\rho_i i_P$, taking into account both northern and southern hemispheres, such that the equatorial radial current i_ρ is

$$i_\rho = \frac{4\Sigma_P^* F\left(\Omega_J - \omega_i\right)}{\rho_e}, \quad (17)$$

where we have used $F = B_J\rho_i^2$ on a flux shell from Eq. (2). We hence find that the total radial current, integrated in azimuth, is

$$I_\rho = 2\pi\rho_e i_\rho = 8\pi\Sigma_P^*\Omega_J F\left(1 - \frac{\omega_i}{\Omega_J}\right), \quad (18)$$

which is equal, of course, to twice the azimuth-integrated Pedersen current in each conjugate ionosphere I_P. The field-aligned current density is then calculated from the divergence of either I_ρ or I_P. Using the former, we have

$$j_{\parallel i} = -\frac{B_J}{2\pi}\frac{dI_\rho}{dF} = -4\Sigma_P^* B_J\Omega_J\frac{d}{dF}\left[F\left(1 - \frac{\omega_i}{\Omega_J}\right)\right], \quad (19)$$

which is the parallel current to be substituted into Eq. (11). Note that in deriving Eq. (19) we have assumed for simplicity that Σ_P^* is a constant quantity.

2.4 Conservation of angular momentum (the Hill-Pontius equation)

The analysis is completed by consideration of conservation of angular momentum of the equatorial plasma. Following Hill (1979) and Pontius (1997), this is described by

$$\frac{d}{dF}\left(\rho_e^2\frac{\omega_e}{\Omega_J}\right) = -\frac{I_\rho}{\dot{M}\Omega_J}, \quad (20)$$

where $\dot{M}$ is the iogenic plasma mass outflow rate, also assumed to be a constant. Substitution of Eq. (18) into Eq. (20) then yields the modified 'Hill-Pontius' equation

$$\frac{d}{dF}\left(\rho_e^2\frac{\omega_e}{\Omega_J}\right) = -\frac{8\pi\Sigma_P^* F}{\dot{M}}\left(1-\frac{\omega_i}{\Omega_J}\right), \tag{21}$$

where we note that the LHS now specifically contains ω_e, the angular velocity of the equatorial plasma, while the RHS, representing the ionospheric torque on the equatorial plasma, contains ω_i.

2.5 Governing equation of the self-consistent problem

There are three equations to be solved; the decoupling equation incorporating Knight's (1973) theory Eq. (11), Eq. (19) for the parallel current, and the Hill-Pontius equation Eq. (21). Substitution of Eq. (19) into Eq. (11) yields

$$\frac{\omega_e}{\Omega_J} = \frac{\omega_i}{\Omega_J} + \frac{4\Sigma_P^* B_J W_{th}}{e j_{\parallel io}}\frac{d^2}{dF^2}\left[F\left(1-\frac{\omega_i}{\Omega_J}\right)\right]. \tag{22}$$

We thus introduce the dimensionless parameter ε given by

$$\varepsilon = \frac{4\Sigma_P^* W_{th}}{e j_{\parallel io} R_J^2}, \tag{23}$$

which for typical Jovian parameters Σ_P^*=0.1 mho, $j_{\parallel io}\approx 0.01\,\mu$A m^{-2}, and W_{th}=2.5 keV, for example, has the value $\varepsilon\approx 1.5\times10^{-5}$. Since the first term in the differential vanishes, Eq. (22) then becomes

$$\frac{\omega_e}{\Omega_J} = \frac{\omega_i}{\Omega_J} - \varepsilon B_J R_J^2\frac{d^2}{dF^2}\left(F\frac{\omega_i}{\Omega_J}\right), \tag{24}$$

where we note that all previous papers cited above have employed the limit $\varepsilon\to 0$, such that $\omega_e\to\omega_i$. Substitution of Eq. (24) into the Hill-Pontius equation Eq. (21) finally yields the governing equation for ω_i

$$\frac{d}{dF}\left(\rho_e^2\frac{\omega_i}{\Omega_J}\right) = -\frac{8\pi\Sigma_P^* F}{\dot{M}}\left(1-\frac{\omega_i}{\Omega_J}\right) + \varepsilon B_J R_J^2\frac{d}{dF}\left[\rho_e^2\frac{d^2}{dF^2}\left(F\frac{\omega_i}{\Omega_J}\right)\right]. \tag{25}$$

This is a third order linear inhomogeneous equation for ω_i, from which ω_e can be obtained from Eq. (24), and the current system and field-aligned voltage from Eqs. (18), (19) and (12).

2.6 Series solution of the governing equation

The general solution of Eq. (25) is the sum of a complementary function which solves the homogeneous equation and contains three arbitrary constants, plus some particular integral. The physical solution which we require here, however, is the particular integral which reduces to our previous solutions in the limit $\varepsilon\to 0$. This solution may be obtained as a power series in ε

$$\left(\frac{\omega_i}{\Omega_J}\right) = \sum_{n=0}^{\infty}\varepsilon^n\left(\frac{\omega_i}{\Omega_J}\right)_{(n)}, \tag{26}$$

where each coefficient $(\omega_i/\Omega_J)_{(n)}$ is a function of F. Substitution of Eq. (26) into Eq. (25) gives

$$\frac{d}{dF}\left(\rho_e^2\sum_{n=0}^{\infty}\varepsilon^n\left(\frac{\omega_i}{\Omega_J}\right)_n\right) = -\frac{8\pi\Sigma_P^* F}{\dot{M}}\left(1-\sum_{n=0}^{\infty}\varepsilon^n\left(\frac{\omega_i}{\Omega_J}\right)_n\right) + B_J R_J^2\frac{d}{dF}\left[\rho_e^2\frac{d^2}{dF^2}\left(F\sum_{n=0}^{\infty}\varepsilon^{n+1}\left(\frac{\omega_i}{\Omega_J}\right)_n\right)\right], \tag{27}$$

from which the required functions are found by equating terms of the same power of ε. For the zeroth order n=0, we have

$$\frac{d}{dF}\left[\rho_e^2\left(\frac{\omega_i}{\Omega_J}\right)_{(0)}\right] = -\frac{8\pi\Sigma_P^* F}{\dot{M}}\left[1-\left(\frac{\omega_i}{\Omega_J}\right)_{(0)}\right], \tag{28}$$

which is just the Hill-Pontius equation solved in previous papers. The solution required is the particular integral for which $(\omega_i/\Omega_J)\to 1$ as $\rho_e\to 0$, i.e. for which the plasma rigidly corotates at small distances. For $n\geq 1$ we have

$$\frac{d}{dF}\left[\rho_e^2\left(\frac{\omega_i}{\Omega_J}\right)_{(n)}\right] = \frac{8\pi\Sigma_P^* F}{\dot{M}}\left[\left(\frac{\omega_i}{\Omega_J}\right)_{(n)}\right] + B_J R_J^2\frac{d}{dF}\left\{\rho_e^2\frac{d^2}{dF^2}\left[F\left(\frac{\omega_i}{\Omega_J}\right)_{(n-1)}\right]\right\}, \tag{29}$$

which is a first order linear inhomogeneous equation for $(\omega_i/\Omega_J)_{(n)}$, in which the inhomogeneous term contains the derivative of the solution of the previous order, $(\omega_i/\Omega_J)_{(n-1)}$. The solutions required of these equations are the particular integrals which satisfy $(\omega_i/\Omega_J)_{(n)}\to 0$ as $\rho_e\to 0$ for all $n\geq 1$. In principle, we can then solve Eqs. (28) and (29) in sequence to any desired order in ε. Here we will obtain solutions up to second order, n=2.

The other parameters of interest are obtained by substitution of Eq. (26) into the appropriate equation and equating powers of ε. Thus, for ω_e we obtain from Eq. (24)

$$\left(\frac{\omega_e}{\Omega_J}\right)_{(0)} = \left(\frac{\omega_i}{\Omega_J}\right)_{(0)}, \tag{30a}$$

and for $n\geq 1$

$$\left(\frac{\omega_e}{\Omega_J}\right)_{(n)} = \left(\frac{\omega_i}{\Omega_J}\right)_{(n)} - B_J R_J^2\frac{d^2}{dF^2}\left[F\left(\frac{\omega_i}{\Omega_J}\right)_{(n-1)}\right]. \tag{30b}$$

The total radial and field-aligned currents follow from Eqs. (18) and (19), respectively. The former is given by the power series

$$I_\rho = \sum_{n=0}^{\infty}\varepsilon^n I_{\rho(n)}, \tag{31a}$$

where

$$I_{\rho(0)} = 8\pi\Sigma_P^*\Omega_J F\left[1-\left(\frac{\omega_i}{\Omega_J}\right)_{(0)}\right], \tag{31b}$$

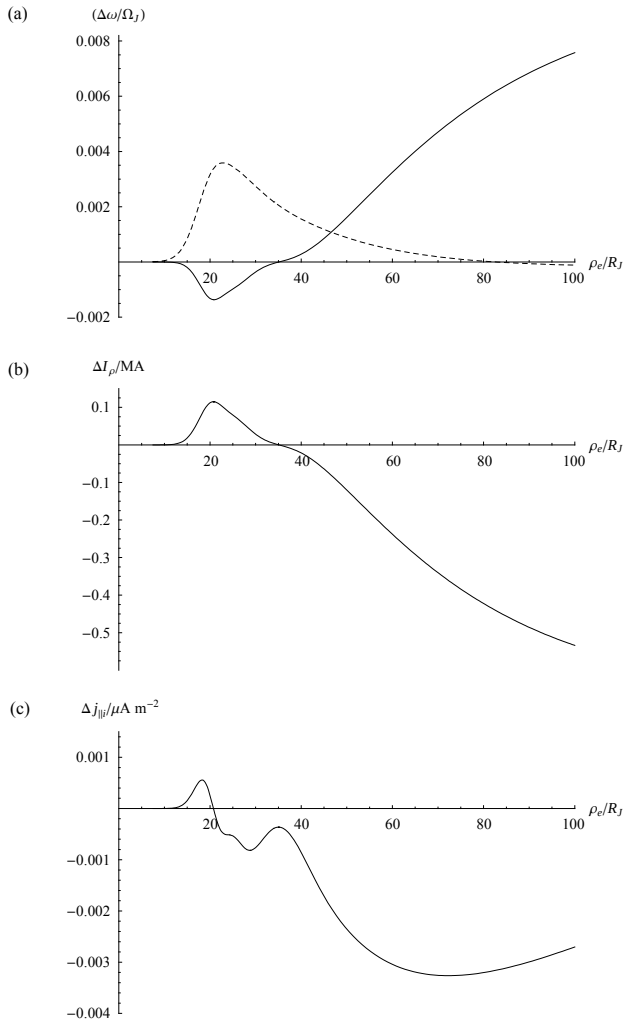

Fig. 3. Plots of the sums of the first and second order terms in the series solutions for **(a)** the normalised equatorial (dashed line) and ionospheric (solid line) plasma angular velocities, **(b)** the total azimuth-integrated equatorial radial current in MA, and **(c)** the ionospheric field aligned current in μA m^{-2}, all plotted versus equatorial radial distance (with ionospheric parameters being mapped along field lines). The system parameters employed were Σ_P^*=0.1 mho and $\dot{M}$=1000 kg s^{-1}, with magnetospheric electron source parameters N=0.01 cm^{-3} and W_{th}=2.5 keV.

and for $n \geq 1$

$$I_{\rho(n)} = -8\pi\,\Sigma_P^*\Omega_J F\left(\frac{\omega_i}{\Omega_J}\right)_{(n)}. \tag{31c}$$

The field-aligned current is similarly given by

$$j_{\parallel i} = \sum_{n=0}^{\infty} \varepsilon^n j_{\parallel i_{(n)}}, \tag{32a}$$

where

$$j_{\parallel i(0)} = -4\Sigma_P^* B_J \Omega_J \frac{d}{dF}\left\{F\left[1-\left(\frac{\omega_i}{\Omega_J}\right)_{(0)}\right]\right\}, \tag{32b}$$

and for $n \geq 1$

$$j_{\parallel i(n)} = 4\Sigma_P^* B_J \Omega_J \frac{d}{dF}\left[F\left(\frac{\omega_i}{\Omega_J}\right)_{(n)}\right]. \tag{32c}$$

Since from Eqs. (12) and (19) we can write

$$\Phi_\parallel = \sum_{n=0}^{\infty} \varepsilon^n \Phi_{\parallel(n)} \approx \varepsilon \frac{R_J^2 j_{\parallel i}}{4\Sigma_P^*} = -\varepsilon B_J R_J^2 \Omega_J \frac{d}{dF}\left[F\left(1-\frac{\omega_i}{\Omega_J}\right)\right] \tag{33a}$$

in the approximation employed here, we have on substituting Eq. (26) for (ω_i/Ω_J)

$$\Phi_{\parallel(0)} = 0, \tag{33b}$$

i.e. to lowest order the parallel voltage is zero as in previous published solutions, while

$$\Phi_{\parallel(1)} = -B_J R_J^2 \Omega_J \frac{d}{dF}\left\{F\left[1-\left(\frac{\omega_i}{\Omega_J}\right)_{(0)}\right]\right\}, \tag{33c}$$

and for $n \geq 2$

$$\Phi_{\parallel(n)} = B_J R_J^2 \Omega_J \frac{d}{dF}\left[F\left(\frac{\omega_i}{\Omega_J}\right)_{(n-1)}\right]. \tag{33d}$$

Hence, if we evaluate (ω_i/Ω_J) and (ω_e/Ω_J) to second order, for example, we can determine the parallel voltage to third order, etc.

With regard to the precipitating energy flux, we have from Eqs. (12) and (13)

$$E_f \approx \frac{E_{f0}}{2}\left(\frac{e\Phi_\parallel}{W_{th}}\right)^2. \tag{34}$$

Thus we express E_f to the same order as $\Phi_\parallel$, such that if we determine the plasma flows to a given order, we can compute the precipitating energy flux to the next highest order.

3 Results

We now present the results of numerical evaluation of the equations in Sect. 2, in order to assess the significance of the effects of field-aligned voltages under typical Jovian conditions. We have used typical values of the system parameters Σ_P^*=0.1 mho and $\dot{M}$=1000 kg s^{-1}, along with magnetospheric electron source parameters N=0.01 cm^{-3} and W_{th}=2.5 keV. For these values we find $\varepsilon \approx 1.5\times10^{-5}$, as indicated above, which is small, such that a power series solution in ε seems appropriate. In Fig. 3 we show the sum of first and second order terms of the series solution for the plasma angular velocity, the azimuth-integrated equatorial radial current, and the ionospheric field-aligned current, all plotted versus distance in the equatorial plane (ionospheric quantities being mapped along the field lines). These represent the amounts by which the previously-published zeroth order solutions are modified by the inclusion of field-aligned voltages (hence the "Δ" notation on the vertical axis labels). The solid line in Fig. 3a shows the change in ionospheric angular velocity

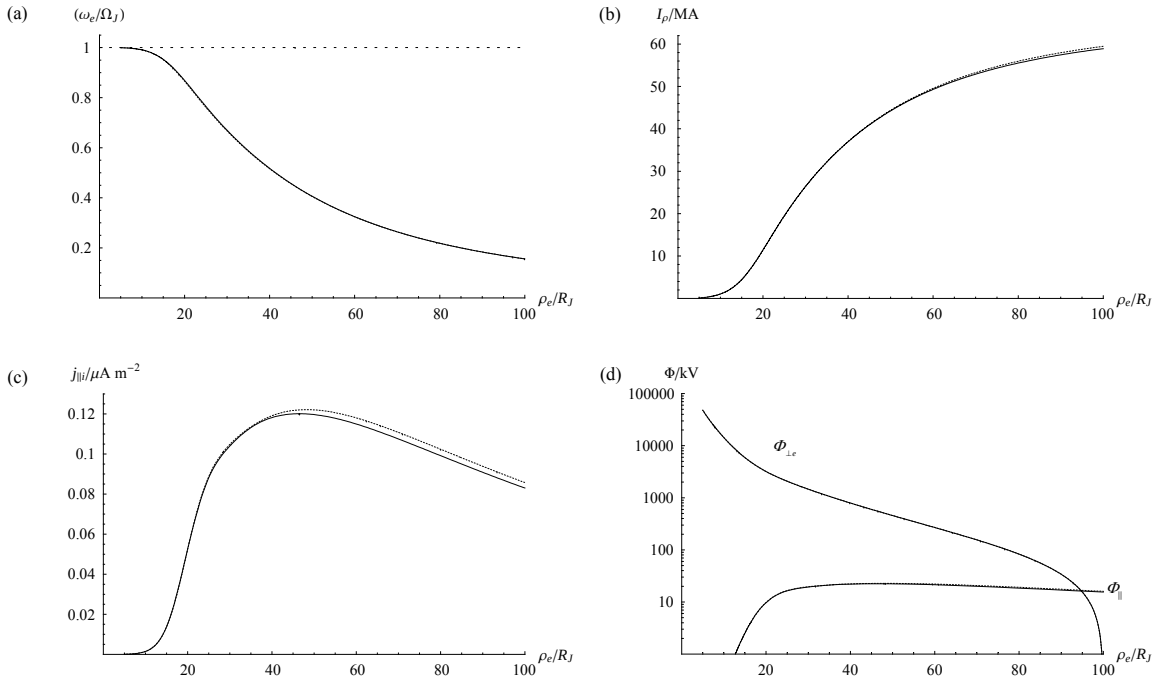

Fig. 4. Plots of the sums of the zeroth, first, and second (and third in the case of the field-aligned voltage) order terms for the system parameters. All parameters are plotted versus equatorial radial distance ρ_e. For comparison, the zeroth order solution alone is shown by the dashed lines. Panel **(a)** shows the normalised equatorial plasma angular velocity, **(b)** the azimuth-integrated equatorial radial current in MA, **(c)** the field-aligned current density in μA m^{-2}, and **(d)** the equatorial electrostatic potential in kV (on a log scale), together with the field-aligned voltage (to third order).

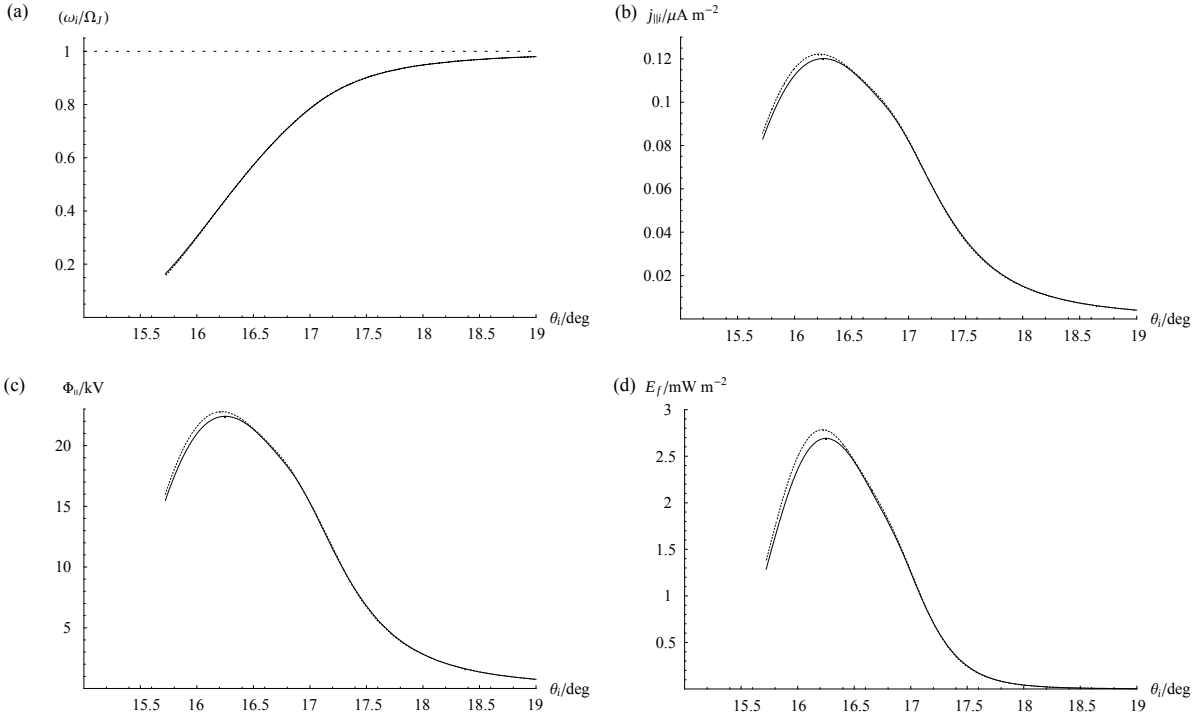

Fig. 5. Plots of the sums of the zeroth, first, and second (and third in the case of the field-aligned voltage) order terms for the system parameters. All parameters are plotted versus ionospheric co-latitude θ_i. For comparison, the zeroth order solution is shown by the short-dashed lines. Panel **(a)** shows the normalised ionospheric plasma angular velocity, **(b)** the field-aligned current density in μA m^{-2}, **(c)** the field-aligned voltage in kV, and **(d)** the precipitating energy flux (calculated from the field-aligned voltage profile shown in panel c) in mW m^{-2}.

$(\Delta\omega_i/\Omega_J)$ calculated from Eq. (29), while the long-dashed line similarly shows the change in the equatorial plasma angular velocity $(\Delta\omega_e/\Omega_J)$ obtained from Eq. (30b). It can be seen that the ionospheric plasma angular velocity will be modestly reduced in the region within $\sim$35 R_J, and elevated thereafter, while the angular velocity of the equatorial plasma will be raised over most of the region. Using techniques introduced by Nichols and Cowley (2003) (see their Eq. 7), it is possible to show that to a first order in ε the solutions for small ρ_e are

$$\left(\frac{\omega_i}{\Omega_J}\right) \simeq 1 - \frac{\dot{M}}{4\pi\,\Sigma_P^* F\,|B_{ze}|} - \ldots \tag{35a}$$

and

$$\left(\frac{\omega_e}{\Omega_J}\right) \simeq 1 - \frac{\dot{M}}{4\pi\,\Sigma_P^* F\,|B_{ze}|} + \frac{\varepsilon\dot{M}}{4\pi\,\Sigma_P^*} B_J R_J^2 \frac{d^2}{dF^2}\left(\frac{1}{|B_{ze}|}\right) - \ldots . \tag{35b}$$

That is, to a first order the ionospheric angular velocity, and hence the current system, is unaffected by the field-aligned voltages. This is because to the lowest order the currents in the inner region are just such as to maintain rigid corotation of the equatorial plasma, and may be deduced by putting $(\omega_e/\Omega_J)=1$ in the LHS of the Hill-Pontius equation, Eq. (20). The equatorial angular velocity is modified to a first order in ε, however, falling less rapidly with distance than when the effect of the field-aligned voltages are neglected. The main point we wish to emphasise with regard to Fig. 3a, however, is that for typical Jovian parameters, the changes in the normalised angular velocity are small compared with unity. The difference in angular velocity between the equatorial plane and the ionosphere due to field-aligned voltage decoupling is typically a few thousandths of the planetary angular velocity. Figure 3b similarly shows the sum of first and second order terms for the azimuth-integrated equatorial radial current ΔI_ρ given by Eq. (31c). The profile essentially mirrors that of the ionospheric angular velocity as expected, such that the current is slightly raised within $\sim$35 R_J and decreased beyond. Figure 3c shows the sum of first and second order terms for the field-aligned current $\Delta j_{\parallel i}$ given by Eq. (32c), mapped to the equatorial plane. It can be seen that the field-aligned current is reduced over most of the middle magnetosphere. We note that the rapid variations of these profiles in the inner region results from the B_{ze} model used, which exhibits rather sharp behaviour at $\sim$20 R_J in the transition region between the dipolar form and the power law (Fig. 2a). Such variations do not occur if a simple dipole model is used, though the overall nature of the results remains similar. We also note that the quantities shown in Fig. 3 are dominated by the first order term, which for all parameters is typically an order of magnitude larger than the second order term.

The effect of including these terms on the overall solution for the angular velocity and currents is shown in Figs. 4 and 5. Figure 4 shows these parameters plotted versus radial distance in the equatorial plane, while Fig. 5 shows profiles mapped along field lines to the ionosphere and plotted versus co-latitude. The solid lines in the figures show the sums of the zeroth, first, and second order terms for the angular velocity and current parameters (i.e. the zeroth order terms summed with the profiles shown in Fig. 3), while the short-dashed lines show the zeroth order terms alone for comparison. Figure 4 shows (a) the equatorial plasma angular velocity (ω_e/Ω_J), (b) the azimuth-integrated equatorial radial current I_ρ, (c) the ionospheric field-aligned current $j_{\parallel i}$, and (d) a log-linear plot of the equatorial electrostatic potential $\Phi_{\perp e}$ computed from the equatorial plasma angular velocity profiles shown in Fig. 4a using

$$\Phi_{\perp e} = \int_F^{F(100R_J)} \omega_e\,(F) dF, \tag{36}$$

where the arbitrary zero of potential is taken to be at the outer edge of the solution at 100 R_J. Also shown in Fig. 4d is the field-aligned voltage $\Phi_\parallel$ computed from the respective orders of the plasma angular velocity using Eqs. (33c, d), such that this is shown to first and third orders by the dashed and solid lines respectively (recalling that the zeroth order field-aligned voltage is zero). It can be seen directly from these plots that the effect of the self-consistent inclusion of the field-aligned voltage in the solution is small. The equatorial angular velocity profiles (and hence the equatorial electrostatic potential profiles) are closely similar, such that their difference cannot be distinguished on this scale, while the magnitudes of the perpendicular and parallel currents are slightly reduced in the outer region, corresponding to the negative values of ΔI_ρ and $\Delta j_{\parallel i}$ in Fig. 3. We also note from Fig. 4d that the drop in $\Phi_{\perp e}$ across the middle magnetosphere, between $\sim$20 R_J and the outer edge of the model at 100 R_J, is $\sim$3 MV. This is approximately two orders of magnitude larger than $\Phi_\parallel$. This formed the basis of Cowley and Bunce's (2001) conjecture that the field-aligned voltage would have little effect on the solutions, as is now confirmed quantitatively here.

Figure 5 similarly shows the system parameters plotted in the ionosphere versus co-latitude. Specifically, we show (a) the ionospheric plasma angular velocity (ω_i/Ω_J), (b) the ionospheric field-aligned current $j_{\parallel i}$, (c) the field-aligned voltage $\Phi_\parallel$ (also shown by the 'lower' line in Fig. 4d), and (d) the precipitating energy flux E_f calculated from the field-aligned voltages shown in Fig. 5c using Eq. (34). As with the equatorial parameters, the effect of the higher order terms is seen to be small. The difference between the ionospheric angular velocity profiles is almost indistinguishable, while the peaks in Figs. 5b, c and d are reduced in amplitude by values approximately two orders of magnitude below the zeroth order results, and are shifted equatorward by $\sim$0.1°, which is small with respect to the $\sim$2° width of the peaks.

4 Summary and conclusion

In this paper we have considered the magnetosphere-ionosphere coupling current system that flows in Jupiter's middle magnetosphere, which is believed to be associated

with the Jovian main auroral oval. Previous analyses have assumed a perfect mapping of the electric field and flow along equipotential field lines between the ionosphere and the magnetosphere, while it is known that substantial field-aligned voltages must exist to drive the currents responsible for the main oval auroras. Cowley and Bunce (2001) suggested that the effect of the field-aligned voltages on the solutions would not be great, but did not compute quantitative results. In this paper we have self-consistently incorporated the field-aligned voltages into the analysis of the system, such that the plasma angular velocities in the magnetosphere and the ionosphere are in general different, with consequences for the currents flowing in the system. The field-aligned voltages were incorporated using Knight's (1973) kinetic theory, and a third order linear inhomogeneous equation for the ionospheric plasma angular velocity was derived (Eq. 25) that can be solved as a power series under appropriate conditions. The zeroth order solution corresponds to those which have been obtained previously, in which there is no decoupling between the ionosphere and magnetosphere. Higher orders then introduce decoupling due to field-aligned voltages, such that the ionospheric and equatorial plasma angular velocity profiles are modified, as are the resulting current profiles. Here the solution has been taken to a second order. The results of numerical evaluation show that, for parameters which are representative of Jovian middle magnetosphere conditions, the decoupling effect of the field-aligned voltages is small. The equatorial and ionospheric plasma angular velocity profiles differ by only a few thousandths of the planetary angular velocity, while the currents, and hence the auroral parameters, are slightly reduced in magnitude by up to a few percent. Our most important conclusion, however, is that our calculations have confirmed the essential validity of previously-published results that did not self-consistently include the decoupling effect of field-aligned voltages in the Jovian middle magnetosphere.

Acknowledgements. J. D. Nichols was supported during the course of this study by a PPARC Quota Studentship, and S. W. H. Cowley by PPARC Senior Fellowship PPA/N/S/2000/00197.

Topical Editor T. Pulkkinen thanks two referees for their help in evaluating this paper.

References

Bagenal, F.: Empirical model of the Io plasma torus, J. Geophys. Res., 99, 11 043–11 062, 1994.

Belcher, J. W.: The low-energy plasma in the jovian magnetosphere, in: Physics of the Jovian Magnetosphere, edited by: Dessler, A. J., Cambridge Univ. Press, Cambridge, UK, 68, 1983.

Bunce, E. J. and Cowley S. W. H.: Divergence of the equatorial current in the dawn sector of Jupiter's magnetosphere: analysis of Pioneer and Voyager magnetic field data, Planet. Space Sci., 49, 1089–1113, doi:10.1016/S0032-0633(01)00004-6 , 2001.

Clarke, J. T., Ballester, G., Trauger, J., Ajello, J., Pryor, W., Tobiska, K., Connerney, J. E. P., Gladstone, G. R., Waite Jr., J. H., Ben Jaffel, L., and Gérard, J.-C.: Hubble Space Telescope imaging of Jupiter's UV aurora during the Galileo orbiter mission, J. Geophys. Res., 103, 20 217–20 l236, doi: 10.1029/98JE01130, 1998.

Connerney, J. E. P., Acuña, M. H., and Ness, N. F.: Modeling the Jovian current sheet and inner magnetosphere, J. Geophys. Res., 86, 8370–8384, 1981.

Connerney, J. E. P., Acuña, M. H., Ness, N. F., and Satoh, T.: New models of Jupiter's magnetic field constrained by the Io flux tube footprint, J. Geophys. Res., 103, 11 929–11 940, doi:10.1029/97JA03726, 1998.

Cowley, S. W. H. and Bunce, E. J.: Origin of the main auroral oval in Jupiter's coupled magnetosphere-ionosphere system, Planet. Space Sci., 49, 1067–1088, doi:10.1016/S0032-0633(00)00167-7, 2001.

Cowley, S. W. H., Nichols, J. D., and Bunce E. J.: Steady-state distributions of flow, current, and auroral precipitation in Jupiter's middle magnetosphere: Solutions for current sheet and dipole magnetic field models, Planet. Space Sci., 50, 717–734, doi:10.1016/S0032-0633(02)00046-6, 2002.

Cowley, S. W. H., Bunce, E. J., and Nichols, J. D.: Origins of Jupiter's main oval auroral emissions, J. Geophys. Res., 108 (A4), 8002, doi:10.1029/2002JA009329, 2003.

Delamere, P. A. and Bagenal, F.: Modeling variability of plasma conditions in the Io torus, J. Geophys. Res., 108 (A7), 1276, doi:10.1029/2002JA009706, 2003.

Dougherty, M. K, Balogh, A., Southwood, D. J., and Smith, E. J.: Field-aligned currents in the jovian magnetosphere during the Ulysses flyby, Planet. Space Sci., 41, 291–300, doi:10.1016/0032-0633(93)90024-V, 1993.

Grodent, D., Clarke, J. T., Kim, J., Waite Jr., J. H., and Cowley, S. W. H.: Jupiter's main oval observed with HST-STIS, J. Geophys. Res., 108 (A11), 1389, doi:10.1029/2003JA009921, 2003.

Hill, T. W.: Inertial limit on corotation, J. Geophys. Res., 84, 6554–6558, 1979.

Hill, T. W.: The jovian auroral oval, J. Geophys. Res., 106, 8101–8108, doi:10.1029/2000JA000302, 2001.

Hill, T. W., Dessler, A. J., and Goertz, C. K.: Magnetospheric models, in: Physics of the Jovian Magnetosphere, edited by: Dessler, A. J., Cambridge Univ. Press, Cambridge, UK, 353, 1983.

Huang, T. S. and Hill, T. W.: Corotation lag of the jovian atmosphere, ionosphere and magnetosphere, J. Geophys. Res., 94, 3761–3765, doi: 10.1029/88JA04306, 1989.

Khurana, K. K.: Influence of solar wind on Jupiter's magnetosphere deduced from currents in the equatorial plane, J. Geophys. Res., 106, 25 999–26 016, doi:10.1029/2000JA000352, 2001.

Khurana, K. K. and Kivelson, M. G.: Inference of the angular velocity of plasma in the jovian magnetosphere from the sweepback of magnetic field, J. Geophys. Res., 98, 67–80, doi:10.1029/92JA01890, 1993.

Knight, S.: Parallel electric fields, Planet. Space Sci., 21, 741–750, doi:10.1016/0032-0633(73)90093-7, 1973.

Lundin, R. and Sandahl, I.: Some characteristics of the parallel electric field acceleration of electrons over discrete auroral arcs as observed from two rocket flights, Symposium on European Rocket Research, ESA SP-135, 125–136, 1978.

Millward, G. H., Miller, S., Stallard, T., Achilleos, N., and Aylward, A. D.: On the dynamics of the jovian ionosphere and thermosphere IV: Ion-neutral coupling, Icarus, 173, 200–211, doi:10.1016/j.icarus.2004.07.027, 2005.

Nichols, J. D. and Cowley, S. W. H.: Magnetosphere-ionosphere coupling currents in Jupiter's middle magnetosphere: Dependence on the effective ionospheric Pedersen conductivity and iogenic plasma mass outflow rate, Ann. Geophys., 21, 1419–1441,

2003,
SRef-ID: 1432-0576/ag/2003-21-1419.

Nichols, J. D. and Cowley, S. W. H.: Magnetosphere-ionosphere coupling currents in Jupiter's middle magnetosphere: Effect of precipitation-induced enhancements of the Pedersen conductivity, Ann. Geophys., 22, 1799–1827, 2004,
SRef-ID: 1432-0576/ag/2004-22-1799.

Pallier, L. and Prangé, R.: More about the structure of the high latitude jovian aurorae, Planet. Space Sci., 49, 1159–1173, doi:10.1016/S0032-0633(01)00023-X, 2001.

Pontius Jr., D. H.: Radial mass transport and rotational dynamics, J. Geophys. Res., 102, 7137–7150, doi:10.1029/97JA00289, 1997.

Prangé, R., Rego, D., Pallier, L., Connerney, J. E. P., Zarka, P., and Queinnec, J.: Detailed study of FUV jovian auroral features with the post-COSTAR HST faint object camera, J. Geophys. Res., 103, 20 195–20 216, doi:10.1029/98JE01128, 1998.

Satoh, T., Connerney, J. E. P., and Baron, R. L.: Emission source model of Jupiter's H_3^+ aurorae: A generalized inverse analysis of images, Icarus, 122, 1–23, doi:10.1006/icar.1996.0106, 1996.

Scudder, J. D., Sittler Jr., E. C., and Bridge, H. S.: A survey of the plasma electron environment of Jupiter: a view from Voyager, J. Geophys. Res., 86, 8157–8179, 1981.

Siscoe, G. L. and Summers, D.: Centrifugally-driven diffusion of iogenic plasma, J. Geophys. Res., 86, 8471–8479, 1981.

Vasavada, A. R., Bouchez, A. H., Ingersoll, A. P., Little, B., and Anger, C. D.: Jupiter's visible aurora and Io footprint, J. Geophys. Res., 104, 27 133–27 142, doi:10.1029/1999JE001055, 1999.

Vasyliunas, V. M.: Plasma distribution and flow, in: Physics of the Jovian Magnetosphere, edited by: Dessler, A. J., Cambridge Univ. Press, Cambridge, UK, 395, 1983.